THIEME OPEN ACCESS

Original Research

Tibial Torsion Malalignment in Small Dogs with Medial Patellar Luxation

Arata Isono[1,2] Yasuji Harada[1] Nobuo Kanno[1] Yasushi Hara[1]

[1] Division of Veterinary Surgery, Department of Veterinary Science, Faculty of Veterinary Medicine, Nippon Veterinary and Life Science University, Musashino-shi, Tokyo, Japan
[2] Otakibashi Animal Hospital, Shinjuku-ku, Tokyo, Japan

Address for correspondence Yasuji Harada, D.V.M., PhD, Division of Veterinary Surgery, Department of Veterinary Science, Faculty of Veterinary MedicineNippon Veterinary and Life Science University, Musashino-shi, Tokyo, Japan (e-mail: yasuji@nvlu.ac.jp).

Vet Comp Orthop Traumatol

Abstract

Objective Medial patellar luxation (MPL) is prevalent in small dogs; however, the causes vary, and few studies have reported tibial deformities. We aimed to conduct a detailed morphological investigation of internal tibial torsion and internal foot rotation and compare the results between MPL grades to better understand the pathogenesis of MPL.

Study Design We performed a morphological study of the tibia and comparison with MPL grade, and established a new parameter, metatarsal orientation relative to the orientation of the tibial tuberosity, the proximal tibia metatarsal angle (PTMTA). The distal tibia metatarsal angle was also established, and tibial torsion angle (TTA), mechanical medial proximal tibial angle, medial distance of the tibial tuberosity/proximal tibial width, and crural rotation angle were compared among the grades of MPL.

Results The PTMTA was significantly higher in grades 3 and 4 than in the normal group. TTA, medial distance of the tibial tuberosity/proximal tibial width, and mechanical medial proximal tibial angle were significantly higher in grade 4 than in the other grades, which is consistent with previous reports. A correlation was also observed between the PTMTA and the TTA.

Conclusion The PTMTA functioned as a parameter that included elements of the distal tibia metatarsal angle, TTA, and medial distance of the tibial tuberosity/proximal tibial width, and is considered clinically useful because it can be visually ascertained during palpation. Our results may play a major role in surgical decision-making in the treatment of MPL.

Keywords

- medial patellar luxation
- small breed dogs
- tibial torsion
- malalignment
- proximal tibia metatarsal angle

Introduction

Medial patellar luxation (MPL) is a common orthopaedic disease in toy breeds. A recent study investigating the pathogenesis thereof performed standing computed tomography (CT) scans of toy poodles with grade 2 MPL and found that their skeletal and postural features included external torsion of femur, internal torsion of the tibia and internal rotation of the foot, external rotation of tarsal joint, a large stifle joint convergence angle, genu varum, and toe-in standing.[1] Several studies have described femoral deformities that induce MPL; however, few have reported tibial deformities.[2–7]

There have been several reports regarding the tibia in MPL in small dogs. Tibial torsion increases with increasing MPL grade in Yorkshire terriers.[8] In 2015, Yasukawa and colleagues performed CT studies on MPL-affected toy poodle cases and showed that the tibial torsion angle (TTA) of MPL

received
November 8, 2023
accepted after revision
October 21, 2024

DOI https://doi.org/10.1055/s-0044-1796628.
ISSN 0932-0814.

Georg Thieme Verlag KG, Oswald-Hesse-Straße 50, 70469 Stuttgart, Germany

grade 4 dogs was significantly higher than that of normal and grade 2 groups.[5] In 2018, Phetkaew and colleagues also performed CT studies Chihuahua cases and showed that MPL grade 4 had a significantly higher TTA than normal and grade 1, 2, and 3 cases.[7] Thus, recent morphological investigations of the tibia using CT have suggested that torsion of the tibia may be involved in MPL pathogenesis.[5,7,8] However, no significant difference in torsion of the tibia was found between grades 2 and 3.[7,8] In addition, studies reported to date have measured the tibia alone, and few reports have described the relationship between the foot and tibial tuberosity orientation.[1,5,7–11]

We aimed to conduct a more detailed morphological investigation of the internal torsion of the tibia and internal rotation of the foot and compared the results between grades to better understand the pathogenesis of MPL. Additionally, we established a new parameter, metatarsal orientation relative to the orientation of the tibial tuberosity, the proximal tibia metatarsal angle (PTMTA), which can be easily visually assessed as a landmark, and performed a correlation with the previously reported TTA. The distal tibia metatarsal angle (DTMTA), which is the orientation of the metatarsal bone relative to the front of the tibia, was also set, and the previously reported mechanical medial proximal tibial angle (mMPTA), medial distance of the tibial tuberosity/proximal tibial width (MDTT/PTW), and crural rotation angle (CRA) were compared between the grades.

Materials and Methods

Patients

The subjects were 76 dogs presented to the Nippon Veterinary and Life Science University and 8 dogs presented to the Otakibashi Animal Hospital between 2017 and 2021 that underwent CT imaging of the hindlimb with no evidence of joint disease other than MPL in the stifle joint. This study was restricted to animals weighing less than 10 kg. This study was conducted with the approval of the director of the hospital, and all owners of the dogs included in this study consented to the collection of data.

We graded the luxation based on Roush's patellar luxation grading system,[12] which is a simplification of Singleton's system that was adapted from Putnam[6]: grade 1, the patella can be manually luxated but returns to a normal position when released; grade 2, the patella can luxate during stifle flexion or manual manipulation and remains luxated until stifle extension or manual replacement occurs; grade 3, the patella is permanently luxated but can be manually replaced; it luxates again spontaneously when manual pressure is removed; and grade 4, the patella is permanently luxated and cannot be replaced. In our study, grades 2 to 4 were included in the analysis. The control group was defined as animals with a stifle joint with no palpable MPL and included 10 contralateral limbs of the affected limb, 2 limbs with transverse spinal cord disease, 2 limbs with pelvic fracture, and 1 limb with hip subluxation.

Methods

The PTMTA, DTMTA, TTA, mMPTA, MDTT/PTW, and CRA were used to measure tibial morphology. Based on previous reports, CT imaging was used for all tibial measurements.[13–17] To reduce differences due to CT imaging positioning, the dogs were placed on their backs with the hip, stifle, and tarsal joints flexed at approximately 90 degrees and the long axes of the right and left femurs parallel to each other, as per previous reports (►**Fig. 1**).[11]

Fig. 1 Images obtained with a slice thickness of 0.5 mm and reconstruction intervals of 0.3 mm of the hip, knee, and tarsal joints flexed at 90 degrees to the body axis, with the right and left femur and metatarsals in the vertical position and the tibia in the horizontal position.

All CT images were acquired using a 16- or 128-slice helical scanner (Toshiba Aquilion, Toshiba Ltd., Tochigi, Japan) and were reconstructed as 3D images using image-processing software (Toshiba Aquilion, Toshiba Ltd.). All images were reconstructed as 3D multiplanar reconstruction images using the Horos image-processing software (Horos Project, United States; version 3.3.6), and each parameter was measured using ImageJ (1.53k, Bethesda, MD, United States) software based on these images.

The tibial torsion angle and CRA were expressed as positive values for the internal torsion of the proximal tibia relative to the distal tibia and as negative values for the external torsion.

Based on previous reports, 12 months after the growth of the proximal tibial growth plate, distal growth plate, and tibial tuberosity had ceased was considered the criterion; patients younger than 12 months at the time of CT imaging were considered to be in the skeletally immature group (group SI) and those $\geq$12 months were in the skeletally matured group (group SM), and each grade and parameter were evaluated.[18–20]

Proximal Tibia Metatarsal Angle and Distal Tibia Metatarsal Angle

Additionally, we established the PTMTA as a new parameter to evaluate tibial torsion malalignment, as the angle created by the proximal tibial landmark oriented toward the tibial tuberosity and the distal landmark oriented toward the third and fourth metatarsal bones.

To measure the PTMTA, we first determined the reference line in the longitudinal tibial direction,[14] drawn by connecting two landmarks: the proximal landmark is the midpoint of the medial and lateral intercondylar tubercles and the distal

point is positioned on the craniodistal intermediate ridge of the tibia (►**Fig. 2A, B**).

►**Fig. 2C** depicts an multiplanar reconstruction image of the tibia slightly more proximal than ►**Fig. 2B**. The details are presented in ►**Fig. 2C**.

To measure the PTMTA, a tibial tuberosity bisecting line was extrapolated (►**Fig. 3A**). The images of the medial tibial tuberosity and the most caudal point of the extensor hallucis longus groove were extrapolated from the axial section of the tibia; the maximum intensity projection was thickened if the tibial tuberosity could not be extracted from a single slice. Point C was defined as the intersection of a straight line along the medial cortical bone of the tibial tuberosity from the medial prominence of the medial collateral ligament attachment (point A), and a straight line along the lateral cortical bone of the lateral tibial tuberosity from the most caudal point of the lateral extensor hallucis longus groove (point B). The bisection point of the ACB angle was designated as the tibial tuberosity bisecting line.

Subsequently, the metatarsal line (ML) was extrapolated (►**Fig. 3B**). First, a tibial axial section in which the long axes of the third and fourth tarsal bones could be observed was delineated (if it could not be extracted in one slice, thickening of the maximum intensity projection was delineated). Straight lines were drawn between the midpoint of the bone width at the distal third of the third metatarsal length (point D) and the midpoint of the bone width at the middle of the third metatarsal length (point E). Another line connected the midpoint of the bone width at the distal third of the fourth metatarsal length (point F) to the midpoint of the bone width at the middle of the fourth metatarsal length (point G; ►**Fig. 3B**). Thereafter, the bisector of the intersection of these two straight lines (point H) was defined as the ML (►**Fig. 3B**), and the angle between the ML and the parallel shift of TTBL' was defined as the PTMTA (►**Fig. 3C, D**). The angle between the ML and the plane defined by the blue line in "a, b, c, and f" was defined as the DTMTA (►**Fig. 3E**). Consistent with the other parameters, internal rotation of the proximal tibia relative to the distal tibia was expressed as a positive value, while external rotation was expressed as a negative value.

Other Outcomes

Other factors, such as MDTT/PTW, mMPTA, TTA, and CRA, were measured according to previous reports.[5,13] In the axial view of the tibia, the ratio of MDTT/PTW was calculated to evaluate the medial displacement of the tibial tuberosity, where PTW is the width of the proximal tibia and MDTT is the distance from the edge of the medial condyle of the tibia to the tibial tuberosity.[5]

The mMPTA was measured in the frontal view of the tibial CT images as the angle formed by reference line and proximal joint orientation line.[5,7,8,11] To evaluate torsion of the tibia, the TTA was calculated as previously described,[5,7,8,11] as the transcondylar angle formed by the transcondylar axis and the cranial tibial axis. The CRA is formed between the caudal tibial line and the malleolar reference line; the caudal tibial line is located at the level of the tibial plateau and the malleolar reference line passes through the craniocaudal center of the medial and lateral malleolar reference lines, which pass through the craniocaudal center of the medial and lateral cochlea (►**Fig. 4**).[13] In this study, torsion was defined as deviation of the bone in the transverse plane within its length, and rotation as deviation at the joint in the transverse plane. Therefore, the term crural torsion angle was used in a previous study, while CRA has been employed in the present study.[13]

Statistical Analysis

Our statistical analyses were performed using SPSS (version 29.0, IBM Corp., Armonk, NY, United States), while multiple regression analysis was performed using STATA 16.0 (Stata Corp). The Kolmogorov–Smirnov normality test was used to evaluate the normality of each item, and one-way analysis of variance was used for comparisons of items with normal distribution. Tukey's multiple comparison test was used as the *post hoc* test. The Dunn–Bonferroni test was used for *post hoc* analyses. The correlation between PTMTA, TTA, and CRA was evaluated using Spearman's rank correlation. In multiple regression analysis, each measurement parameter was set as the dependent variable, while age, body weight, sex, breeds, and grade were designated as explanatory variables. Thereafter, we conducted a *post hoc* analysis to confirm the normality of the residues. The results were considered significant at $p < 0.05$. The mean ± standard deviation was calculated for each grade.

Results

Of the 84 affected hindlimbs that underwent CT imaging between 2017 and 2021, 74 were evaluated after exclusions. The breeds of dogs were as follows: Toy Poodle, 18 limbs; Chihuahua, 15 limbs; Pomeranian, 12 limbs; Yorkshire Terrier, 6 limbs; Maltese, 3 limbs; Cavalier, 2 limbs; Kooikerhondje, 2 limbs; Shiba, 2 limbs; Jack Russell Terrier, 2 limbs; Shih Tzu, 2 limbs; Boston Terrier, 2 limbs; Shetland Sheepdog, 1 limb; and 7 limbs from mixed breeds. Less than three limbs were classified as other. There were 14 male limbs, 18 neutered male limbs, 18 female limbs, and 24 spayed female limbs. The affected limbs included 39 from the right side and 35 limbs from the left. The mean age was 4.6 ± 3.8 years (range, 0.6–14.3 years) and the mean weight was 4.0 ± 2.0 kg (range, 1.8–9.6 kg). Hindlimbs with MPL were graded, as per Roush and colleagues,[15] as grades 2 ($n = 9$), 3 ($n = 31$), and 4 ($n = 19$). The controls had normal hindlimbs ($n = 15$) with no skeletal abnormalities in the stifle and tarsal joints. The breeds in control were Toy Poodle, 4 limbs; Chihuahuas, 2 limbs; Yorkshire terrier, 1 limb; others, 7 limbs; and mix, 1 limb. There were 3 male limbs, 5 neutered male limbs, 2 female limbs, and 5 spayed female limbs; the mean age was 5.8 ± 4.1 years; and the mean weight was 5.0 ± 2.6 kg. The breeds in grade 2 were Chihuahuas, four limbs; Pomeranian, four limbs; and others, one limb. There were 1 male limb, 2 neutered male limbs, 2 female limbs, and 4 spayed female limbs; the mean age was 3.3 ± 3.0 years; and the mean weight was 4.1 ± 1.6 kg. The breeds in grade 3 were Toy Poodle, 6 limbs; Chihuahuas, 6 limbs; Pomeranian, 5 limbs;

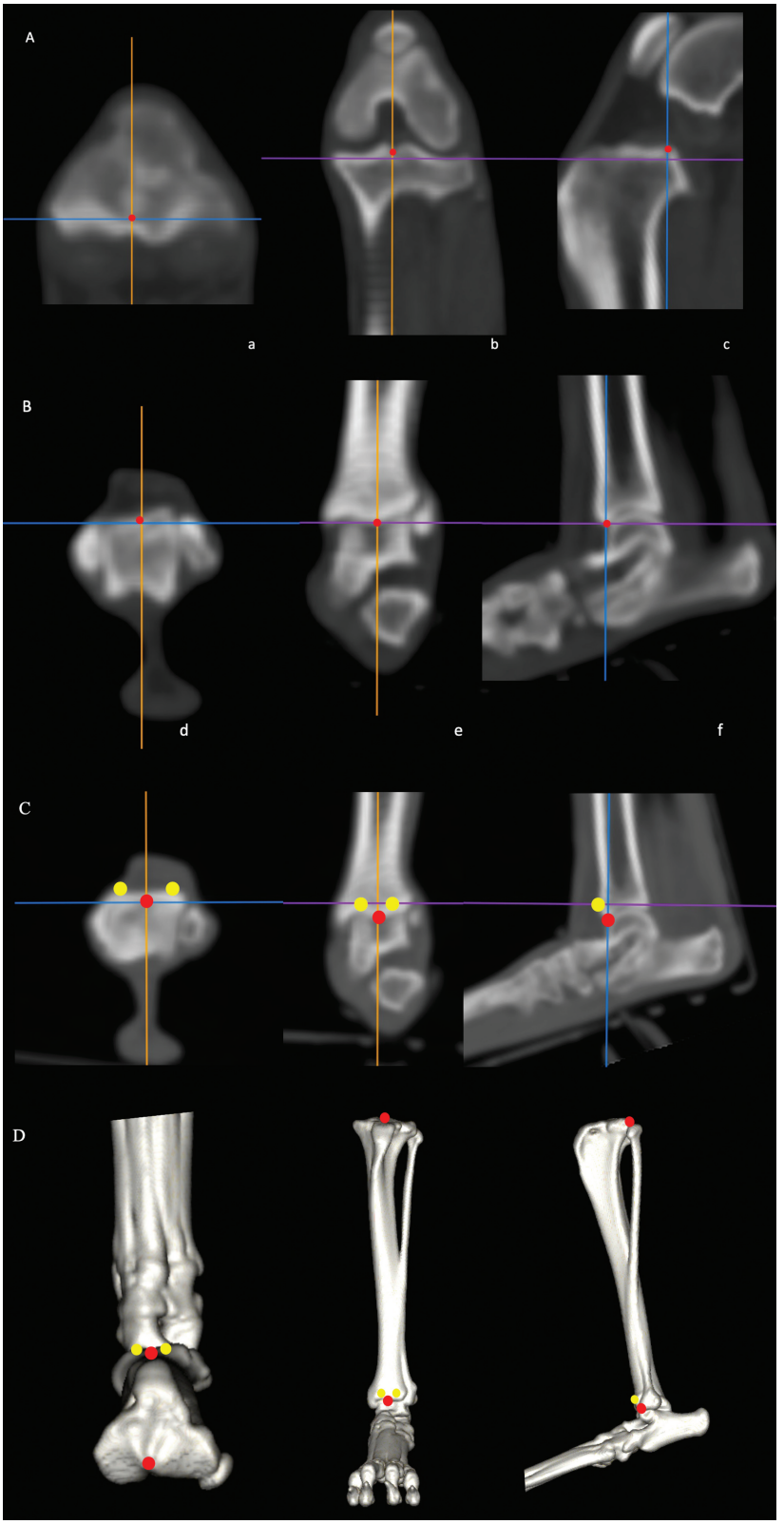

Fig. 2 (**A**) The proximal tibial landmark is the middle of the intercondylar ridge on the medial and lateral sides. a, *purple line*, axial; b, *blue line*, frontal; c, *orange line*, sagittal. (**B**) The distal tibial landmark is the distal ridge of the tibial head. d, *purple line*, axial; e, *blue line*, coronal; f, *orange line*, sagittal. (**C**) A multiplanar reconstruction image of the tibia slightly more proximal than (**B**). The two innermost and outermost points on the flat surface of the tibial isthmus were determined, and the image with a single point was designated the lateral image and the plane perpendicular to it the sagittal plane (*orange plane*). (**D**) A three-dimensional image. The plane defined by the *blue lines* in "a, d, c, and f" is the axial plane. The plane defined by the *orange lines* in "a, d, b, and e" is the sagittal plane. The plane defined by the *purple lines* in "b, e, c, f" is the coronal plane.

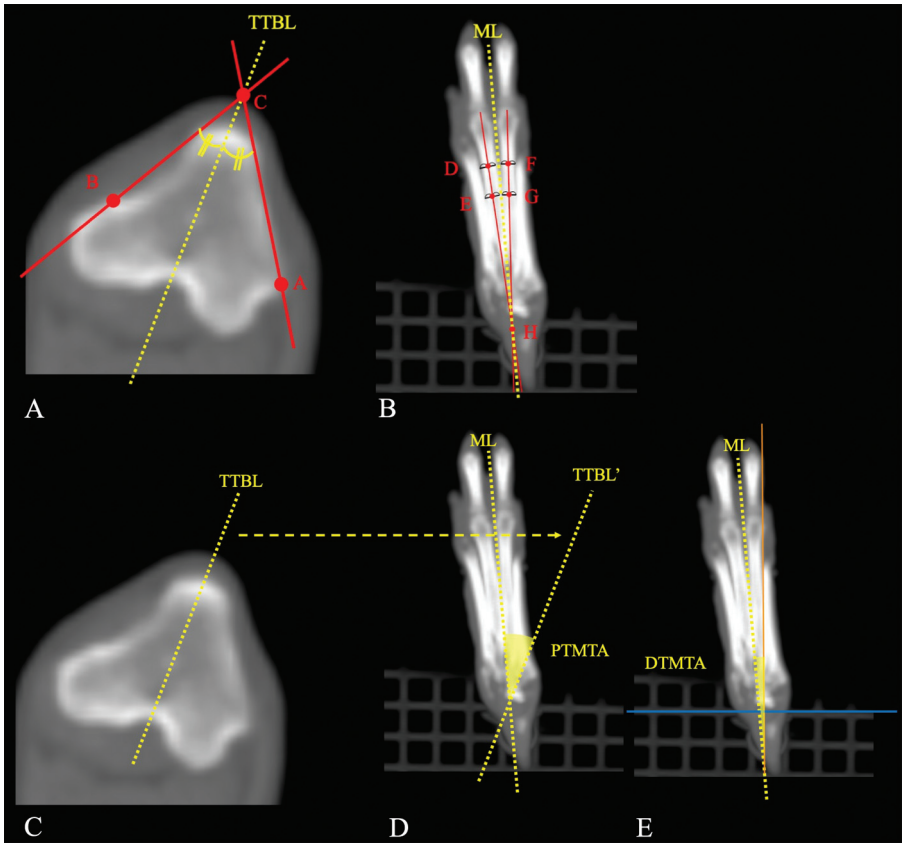

Fig. 3 Images of the left hindlimb. (**A**) The tibial tuberosity bisecting line (TTBL). A straight line is drawn along the medial tuberosity ridge of the tibia (point A), the attachment site of the proximal medial collateral ligament of the tibia, and the medial cortical bone of the tibial tuberosity and the lateral extensor hallucis longus groove (point B). The bisector of the angle between the intersection of these lines and point C is defined as the TTBL. (**B**) Metatarsal line (ML), the line connecting the midpoint of the bone width at the distal third of the third metatarsal length (point D) and the midpoint of the bone width (point E) and the midpoint of the bone width at the distal third of the fourth metatarsal length (point F) and the midpoint of the bone width (point C) are drawn. A straight line connecting the midpoint of the bone width at the distal third of the fourth metatarsal length (point F) and the midpoint of the bone width (point G) is drawn, and the bisector of the intersection of the two straight lines (point H) is defined as the ML. (**C**) Tibial-metatarsal angle distal tibia metatarsal angle (DTMTA), the angle between the ML and the tibial long-axis reference line. The angle between the ML and tibial long-axis reference line is defined as the tibial-metatarsal angle DTMTA. (**D**) Proximal tibia metatarsal angle (PTMTA); the TTBL' is defined as the parallel shift of TTBL, and the angle between the ML and TTBL. The angle between ML and TTBL' is defined as PTMTA, with TTBL' in the medial direction relative to ML expressed as positive and TTBL' in the lateral direction as negative.

Yorkshire terrier, 5 limbs; others, 5 limbs; and mix, 4 limbs. There were 6 male limbs, 9 neutered male limbs, 4 female limbs, and 11 spayed female limbs; the mean age was 5.5 ± 3.9 years; and the mean weight was 3.9 ± 1.8 kg. The breeds in grade 4 were Toy Poodle, 8 limbs; Chihuahuas, 3 limbs; Pomeranian, 3 limbs; others, 3 limbs, and mix 2 limbs. There were 4 male limbs, 2 neutered male limbs, 9 female limbs, and 4 spayed female limbs; the mean age was 2.7 ± 2.6 years; and the mean weight was 3.1 ± 1.3 kg.

The PTMTA tended to increase with increasing severity from normal, grade 2, grade 3, to grade 4, with mean ± standard deviation as follows: normal, 7.1 ± 5.2; grade 2, 8.8 ± 4.3 degrees; grade 3, 13.3 ± 6.7 degrees; and grade 4, 32.8 ± 17.2 degrees. There was a significant difference between the normal and grade 3, normal and grade 4, grade 2 and grade 4, and grade 3 and grade 4 groups ($p < 0.05$).

The mean ± standard deviation of the DTMTA for normal, grade 2, grade 3, and grade 4 was -5.1 ± 3.9, -6.0 ± 3.1,-- 6.9 ± 3.9, and -16.7 ± 7.8 degrees, respectively. Grade 4 was significantly lower than the other grades ($p < 0.05$).

The mean ± standard deviation of the TTA for normal, grade 2, grade 3, and grade 4 was 11.3 ± 4.3, 12.4 ± 7.1, 12.9 ± 5.7, and 21.8 ± 8.6 degrees, respectively. The TTA tended to increase with increasing grade, with significant differences between normal and grade 4, grade 2 and grade 4, and grade 3 and grade 4 ($p < 0.05$).

The mean ± standard deviation of CRA for normal, grade 2, grade 3, and grade 4 was 8.7 ± 5.6, 11.5 ± 3.8, 11.0 ± 4.4, and 19.5 ± 8.0 degrees, respectively. The CRA results revealed significant differences between normal and grade 4, grade 2 and grade 4, and grade 3 and grade 4 ($p < 0.05$). The mean ± standard deviation of the MDTT/PTW for normal, grade 2, grade 3, and grade 4 was 0.51 ± 0.04, 0.50 ± 0.03, 0.49 ± 0.03, and 0.44 ± 0.06, respectively. The mean ± standard deviation of the mMPTA for normal, grade 2, grade 3, and grade 4 was 94.4 ± 2.7, 94.4 ± 1.9, 95.4 ± 2.5, and 100.4 ± 4.0 degrees, respectively. Significant differences were also found for the MDTT/PTW and mMPTA between normal and grade 4, grade 2 and grade 4, and grade 3 and grade 4 ($p < 0.05$ for both; ►**Table 1**).

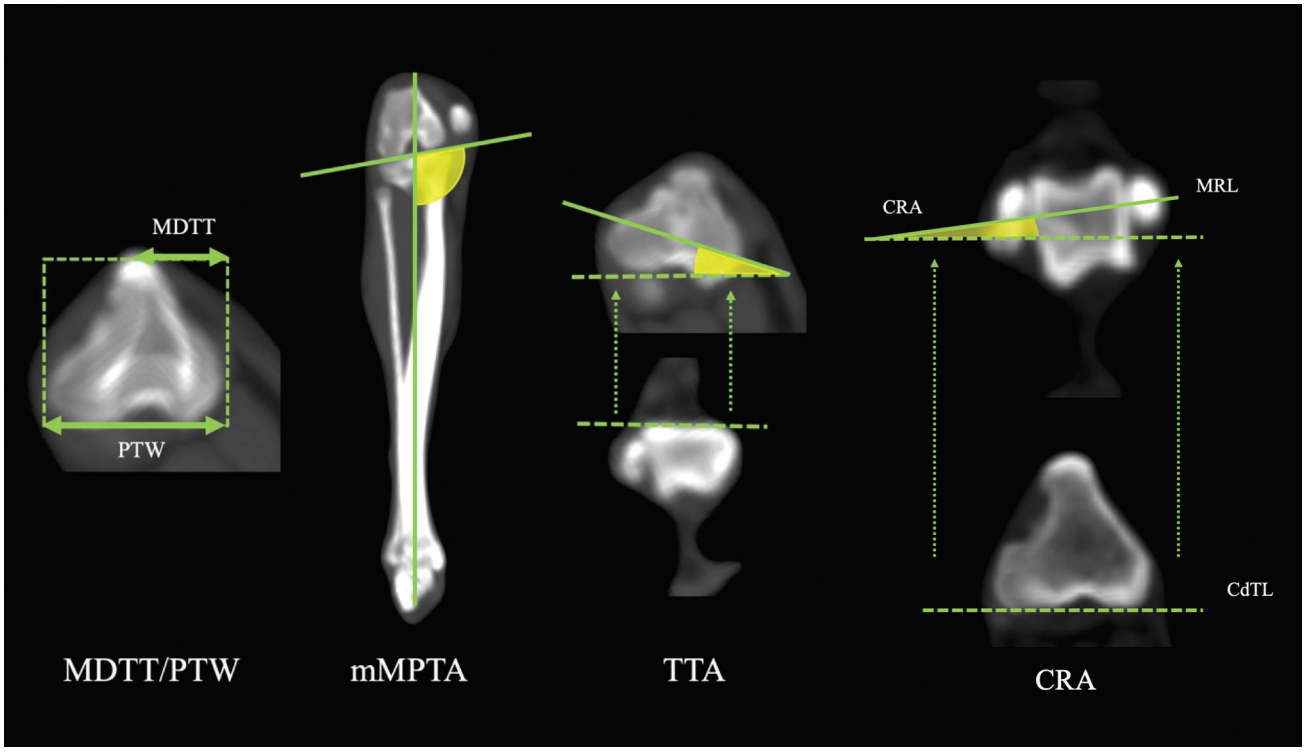

Fig. 4 The mechanical medial proximal tibial angle (mMPTA) is the angle formed by the reference line and the proximal joint orientation line. The tibial torsion angle (TTA) is the angle formed by the transcondylar axis and the cranial tibial axis. The proximal tibial width (PTW) is the width of the proximal tibia; the medial distance of tibial tuberosity (MDTT) is the distance from the edge of the medial condyle of the tibia to the tibial tuberosity. MDTT/PTW is MDTT divided by PTW. The crural rotation angle (CRA) is defined as the angle formed by the caudal tibial line (CdTL) and malleolar reference line (MRL).

Table 1 Measurement values for the tibia

	Normal	Grade 2	Grade 3	Grade 4
Number	15	9	31	19
PTMTA	7.1 ± 5.2^{cd}	8.8 ± 4.3^{d}	13.3 ± 6.7^{ad}	32.8 ± 17.2^{abc}
DTMTA	-5.1 ± 3.9^{d}	-6.0 ± 3.1^{d}	-6.9 ± 3.9^{d}	-16.7 ± 7.8^{abc}
TTA	11.3 ± 4.3^{d}	12.4 ± 7.1^{d}	12.9 ± 5.7^{d}	21.8 ± 8.6^{abc}
CRA	8.7 ± 5.6^{d}	11.5 ± 3.8^{d}	11.0 ± 4.4^{d}	19.5 ± 8.0^{abc}
MDTT/PTW	0.51 ± 0.04^{d}	0.50 ± 0.03^{d}	0.49 ± 0.03^{d}	0.44 ± 0.06^{abc}
mMPTA	94.4 ± 2.7^{d}	94.4 ± 1.9^{d}	95.4 ± 2.5^{d}	100.4 ± 4.0^{abc}

Abbreviations: CRA, crural rotation angle; DTMTA, distal tibia metatarsal angle; MDTT/PTW, medial distance of the tibial tuberosity/proximal tibial width; mMPTA, mechanical medial proximal tibial angle; PTMTA, proximal tibia metatarsal angle; TTA, tibial torsion angle.
Note: Within the same row, lowercase superscript letters indicate significant differences between grades ($p < 0.05$; [a]vs. normal; [b]vs. grade 2; [c]vs. grade 3; [d]vs. grade 4).

There was a significant correlation between the PTMTA and the TTA, and between the PTMTA and the CRA ($p < 0.05$). The correlation coefficient was 0.733 between the PTMTA and the TTA and 0.643 between the PTMTA and the CRA (►**Fig. 5**).

The mean values and standard deviations were determined for each measure and for each grade, classified as group SI and group SM. Further details are presented in ►**Appendix Table A1** (available in the online version). The scatter plots of age and each parameter showed that among the grade 4 groups, younger age at CT imaging tended to have higher PTMTA, DTMTA, TTA, CRA, and mMPTA, and lower MDTT/PTW (►**Fig. 6**).

Multiple regression analysis was performed with each parameter as an independent variable, with the aim of investigating the influence of age, weight, sex, breed, and grade on each parameter. The detailed results are presented in ►**Appendix Table A2** (available in the online version). Multiple regression analysis was conducted with PTMTA as the independent variable in toy poodles with the aim of investigating the effects of age, weight, sex, breed, and grade on PTMTA in toy poodles. The detailed results are presented in ►**Appendix Table A3** (available in the online version).

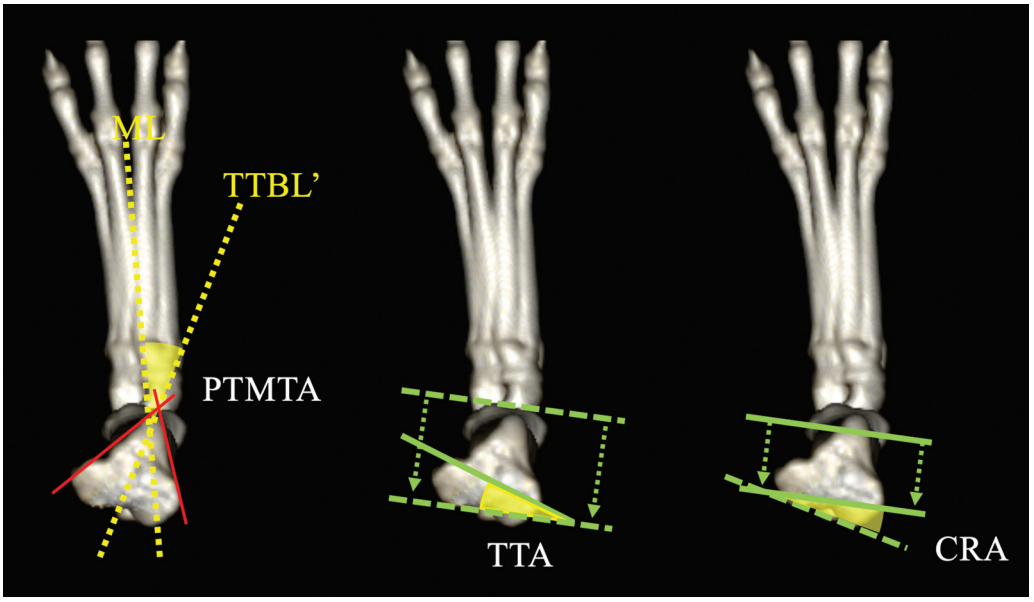

Fig. 5 There was a significant correlation between the proximal tibia metatarsal angle (PTMTA) and the tibial torsion angle (TTA), and between the PTMTA and the crural rotation angle (CRA; $p < 0.05$). The correlation coefficient was 0.733 between the PTMTA and the TTA and 0.643 between the PTMTA and the CRA. ML, metatarsal line; TTBL', parallel shift of the tibial tuberosity bisecting line.

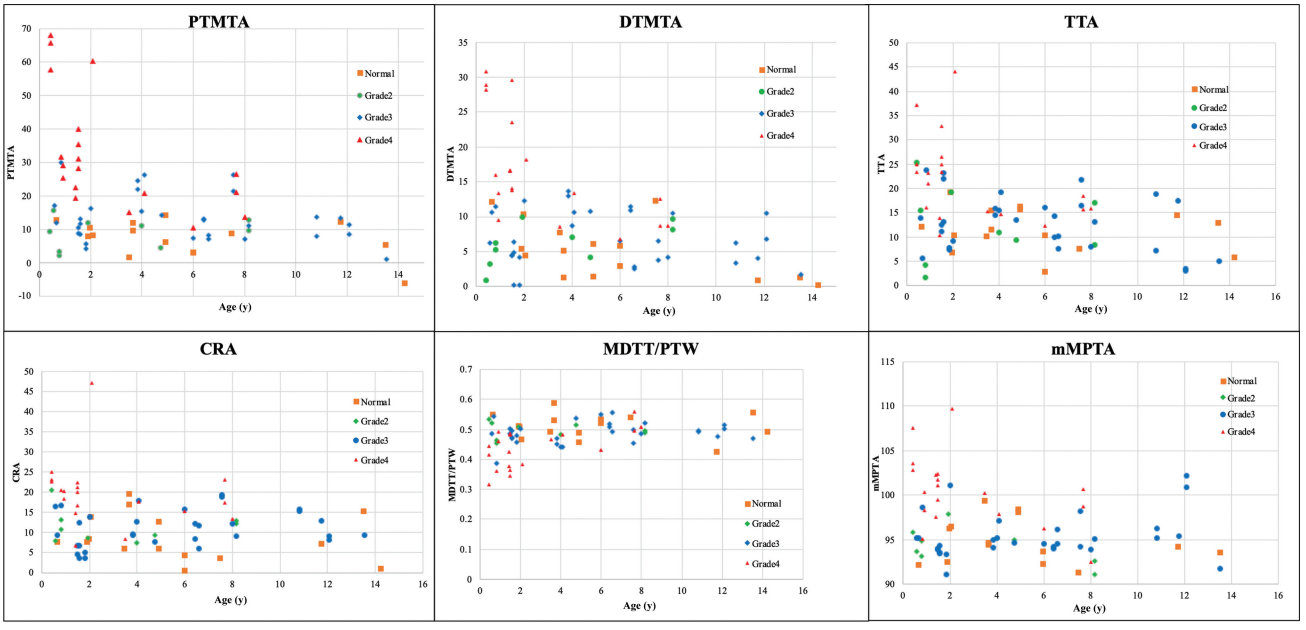

Fig. 6 The scatter plots of age. Grade 1 is indicated by an *orange square*, grade 2 by a *green circle*, grade 3 by a *blue diamond shape*, and grade 4 by a *red triangle*. Each parameter showed that among the four groups, younger age at computed tomography imaging tended to have a higher proximal tibia metatarsal angle (PTMTA), distal tibia metatarsal angle (DTMTA), tibial torsion angle (TTA), crural rotation angle (CRA), and mechanical medial proximal tibial angle (mMPTA), and lower medial distance of tibial tuberosity/ proximal tibial width (MDTT/PTW).

Discussion

We performed a morphological investigation of the internal deviation of tibial metatarsal malalignment by setting and measuring the PTMTA. The tibial deformities showed a trend toward progressively greater internal rotation of the proximal tibia with increasing grade. In our study, grade 4 MDTT/PTW was significantly lower than that of the other grades, which is consistent with another study.[5] In our grade 4 cases, we found a combination of tibial torsion deformity and of simultaneous medial migration of the tibial tuberosity. In the present study, the TTA and MDTT/PTW showed significant differences between grade 4 and the other groups. In contrast, the PTMTA showed significant differences between grade 4 and the other groups and between grade 3 and normal, suggesting that the PTMTA functions as a parameter that incorporates elements of the DTMTA, TTA, and MDTT/PTW, and thus reflects a comprehensive assessment of the severity of the disease.

The PTMTA showed a trend similar to the TTA reported previously, and a correlation was also observed. Recently,

with description of CT imaging techniques for limb alignment in the dog, objective observation and study of skeletal abnormalities associated with MPL have been reported, and the usefulness of CT imaging has been confirmed.[4,5,8,10,14] Computed tomography imaging is necessary to measure the TTA; however, the PTMTA can be visually detected during palpation and is thus clinically useful.[5] The results of this study suggest that evaluating the PTMTA at the time of palpation can provide a preoperative understanding of the morphological characteristics of the tibia, tarsus, and metatarsus.

Although there are reports that the mMPTA is associated with the pathogenesis of MPL, the present validation showed a significant increase only in grade 4.[5,21]

Among our Grade 4 measurements, there were cases with severe PTMTA deformities of $\geq$40 degrees, and in those cases, not only PTMTA deformities but also MDTT/PTW and mMPTA deformities were severe. The grade 4 mMPTA values greater than 100 degrees were so curved that the proximal sagittal plane did not coincide with the distal sagittal plane of the tibia. Although a measurement method exists, it is different from others, and no measurement method exists for torsion and rotation in such cases.[22]

In grade 4, there were six limbs in the SI group, a similar trend to previous reports[18]; however, it is possible that some cases required CT scans at a young age owing to severity of the condition. Thus, the number of patients should be increased in future studies.

The multiple regression analysis model found no significant difference in PTMTA grade 3 compared to normal, but in the investigation in toy poodles, a significant difference was observed between grade 3 and normal, which was considered to be induced by the poodle's grade 3. In the present study, the significant difference in the PTMTA, DTMTA, and MDTT/PTW in toy poodles was also attributed to the high number of toy poodles with severe disease.

Corrective osteotomy has been reported as a treatment option for MPL using anatomical lateral distal femoral angle and other femoral indicators, and some cases have been reported.[18,23–29] No criteria for corrective osteotomy for the tibia have been proposed, and there are few specific reports thereof.[9] The results of the present study provide the necessary tibial morphological information for corrective osteotomy of the MPL.

Our study had some limitations, namely the small number of dogs and the lack of breed identification. Future studies are needed to understand the differences among various breeds. Although imaging was performed based on previous studies, the range of motion beyond the tarsal joint was not evaluated, which may have been influenced by the imaging method.[11] In addition, MPL grade 1 was not examined, and future studies are needed for this grade.

Conclusion

The PTMTA measured in this study correlated with the TTA, confirming its involvement in MPL severity. The correlation with the severity grade was more pronounced than with the TTA, suggesting that the addition of the PTMTA to MPL severity classifications in the future may make it easier to evaluate tibial morphology and may be an auxiliary factor in determining the surgical procedure. In addition, it is necessary to discuss what surgical treatment methods, including corrective osteotomy, would be appropriate for surgical treatment of animals with high PTMTA levels.

Athors' Contribution

A.I. contributed to the conception, study design, acquisition of data, data analysis and interpretation. Y. Harada and Y. Hara contributed to the conception, study design, data analysis and interpretation. N.K. and Y.N. contributed to the conception, acquisition of data, data analysis and interpretation. All authors drafted, revised, and approved the submitted manuscript and are publicly responsible for the relevant content.

Conflict of Interest

None declared.

References

1 Tomo Y, Edamura K, Yamazaki A, et al. Evaluation of hindlimb deformity and posture in dogs with grade 2 medial patellar luxation during awake computed tomography imaging while standing. Vet Comp Orthop Traumatol 2022;35(03):143–151
2 Žilinčík M, Hluchý M, Takáč L, Ledecký V Comparison of radiographic measurements of the femur in Yorkshire terriers with and without medial patellar luxation. Vet Comp Orthop Traumatol 2018;31(01):17–22
3 Di Dona F, Della Valle G, Fatone G. Patellar luxation in dogs. Vet Med (Auckl) 2018;9:23–32
4 Towle HA, Griffon DJ, Thomas MW, Siegel AM, Dunning D, Johnson A. Pre- and postoperative radiographic and computed tomographic evaluation of dogs with medial patellar luxation. Vet Surg 2005;34(03):265–272
5 Yasukawa S, Edamura K, Tanegashima K, et al. Evaluation of bone deformities of the femur, tibia, and patella in Toy Poodles with medial patellar luxation using computed tomography. Vet Comp Orthop Traumatol 2016;29(01):29–38
6 Perry KL, Déjardin LM. Canine medial patellar luxation. J Small Anim Pract 2021;62(05):315–335
7 Phetkaew T, Kalpravidh M, Penchome R, Wangdee C. A comparison of angular values of the pelvic limb with normal and medial patellar luxation stifles in Chihuahua dogs using radiography and computed tomography. Vet Comp Orthop Traumatol 2018;31(02):114–123
8 Fitzpatrick CL, Krotscheck U, Thompson MS, Todhunter RJ, Zhang Z. Evaluation of tibial torsion in Yorkshire Terriers with and without medial patellar luxation. Vet Surg 2012;41(08):966–972
9 Longo F, Nicetto T, Knell SC, Evans RB, Isola M, Pozzi A. Three-dimensional volume rendering planning, surgical treatment, and clinical outcomes for femoral and tibial detorsional osteotomies in dogs. Vet Surg 2022;51(07):1126–1141
10 Aghapour M, Bockstahler B, Vidoni B. Evaluation of the femoral and tibial alignments in dogs: a systematic review. Animals (Basel) 2021;11(06):1804
11 Lusetti F, Bonardi A, Eid C, Brandstetter de Belesini A, Martini FM. Pelvic limb alignment measured by computed tomography in purebred English Bulldogs with medial patellar luxation. Vet Comp Orthop Traumatol 2017;30(03):200–208
12 Roush JK. Canine patellar luxation. Vet Clin North Am Small Anim Pract 1993;23(04):855–868

13 Barnes DM, Anderson AA, Frost C, Barnes J. Repeatability and reproducibility of measurements of femoral and tibial alignment using computed tomography multiplanar reconstructions. Vet Surg 2015;44(01):85–93
14 Longo F, Nicetto T, Pozzi A, Contiero B, Isola M. A three-dimensional computed tomographic volume rendering methodology to measure the tibial torsion angle in dogs. Vet Surg 2021;50(02): 353–364
15 Hette K, Anderson AA, Barnes DM. Assessing torsion of the medial cortex of the canine tibia using computed tomography multiplanar reconstruction. J Small Anim Pract 2016;57(05):234–239
16 Aper R, Kowaleski MP, Apelt D, Drost WT, Dyce J. Computed tomographic determination of tibial torsion in the dog. Vet Radiol Ultrasound 2005;46(03):187–191
17 DeCamp CE, Johnston SA, Dejardin LM, Schaefer S. Brinker, Piermattei, and Flo's Handbook of Small Animal Orthopedics and Fracture Repair. 5th ed. St. Louis, MO: Saunders; 2016:597–669
18 Nagahiro Y, Murakami S, Kamijo K, et al. Segmental femoral ostectomy for the reconstruction of femoropatellar joint in dogs with grade IV medial patellar luxation. Vet Comp Orthop Traumatol 2020;33(04):287–293
19 von Pfeil DJ, DeCamp CE. The epiphyseal plate: physiology, anatomy, and trauma. Compend Contin Educ Vet 2009;31(08): E1–E11, quiz E12
20 Sumner-Smith G. Observations on epiphyseal fusion of the canine appendicular skeleton. J Small Anim Pract 1966;7(04):303–311
21 Bound N, Zakai D, Butterworth SJ, Pead M. The prevalence of canine patellar luxation in three centres. Clinical features and radiographic evidence of limb deviation. Vet Comp Orthop Traumatol 2009;22(01):32–37
22 Walmsley D, Fitzpatrick N, Black C. Correction of biapical tibial deformity by true spherical osteotomy, modified circular external skeletal fixation and distraction osteogenesis. VCOT Open 2019; 02:e73–e80
23 Swiderski JK, Palmer RH. Long-term outcome of distal femoral osteotomy for treatment of combined distal femoral varus and medial patellar luxation: 12 cases (1999-2004). J Am Vet Med Assoc 2007;231(07):1070–1075
24 Hall EL, Baines S, Bilmont A, Oxley B. Accuracy of patient-specific three-dimensional-printed osteotomy and reduction guides for distal femoral osteotomy in dogs with medial patella luxation. Vet Surg 2019;48(04):584–591
25 Brower BE, Kowaleski MP, Peruski AM, et al. Distal femoral lateral closing wedge osteotomy as a component of comprehensive treatment of medial patellar luxation and distal femoral varus in dogs. Vet Comp Orthop Traumatol 2017;30(01):20–27
26 Olimpo M, Piras LA, Peirone B, Fox DB. Comparison of osteotomy technique and jig type in completion of distal femoral osteotomies for correction of medial patellar luxation. An *in vitro* study. Vet Comp Orthop Traumatol 2017;30(01):28–36
27 Panichi E, Cappellari F, Olimpo M, et al. Distal femoral osteotomy using a novel deformity reduction device. Vet Comp Orthop Traumatol 2016;29(05):426–432
28 Hans EC, Kerwin SC, Elliott AC, Butler R, Saunders WB, Hulse DA. Outcome following surgical correction of grade 4 medial patellar luxation in dogs: 47 stifles (2001–2012). J Am Anim Hosp Assoc 2016;52(03):162–169
29 Roch SP, Gemmill TJ. Treatment of medial patellar luxation by femoral closing wedge ostectomy using a distal femoral plate in four dogs. J Small Anim Pract 2008;49(03):152–158

